SSRG International Journal of Electrical and Electronics Engineering
ISSN: 2348-8379/ https://doi.org/10.14445/23488379/IJEEE-V13I3P108

Volume 13 Issue 3, 95-112, March 2026

Original Article

Misalignment Tolerant Inductive Power Transfer System for CC/CV Operation Using PWM Controlled Capacitor

Praveen Manoharan[1], Balaji Chandrasekar[2]*

[1,2]*Department of Electrical and Electronics Engineering, SRM Institute of Science and Technology, Kattankulathur, Chennai, Tamil Nadu, India.*

**Corresponding Author : balajic@srmist.edu.in*

Received: 08 December 2025 Revised: 09 January 2026 Accepted: 12 February 2026 Published: 31 March 2026

Abstract - *In recent years, the Inductive Power Transfer (IPT) system has gained momentum in the electric vehicle and consumer electronics industry. The IPT output system is mainly affected by load variations, misalignment, and environmental factors. A novel approach is presented in this article to reduce the impact of those factors on Constant Voltage (CC)/Constant Current (CV) charging in the IPT system. The compensation capacitor in the Series-Series (SS) compensation is replaced by the Pulse Width Modulation Controlled Capacitor (PWMCC). PWMCC varies its capacitance in real-time to maintain the CC/CV operation regardless of misalignment, load changes, and aging. The MOSFET duty ratio is varied in the PWMCC to obtain the desired capacitance. With the simple SS compensation, the proposed IPT system operates under two different resonant conditions by maintaining fixed frequency operation for achieving CC/CV operation. In the simulation, the misalignment is realized by varying the mutual inductance. The simulation and experimental investigations have been carried out for a 500W system, and the results are presented to validate the theoretical analysis. Lastly, the proposed system is compared with similar works reported recently.*

Keywords - *Inductive Power Transfer, Misalignment Tolerance, PWM Controlled Capacitor, Constant Current/Voltage Charging, Series-Series Compensation.*

1. Introduction

Currently, there is a trend toward using Inductive Power Transfer (IPT) systems in all types of electrically charged vehicles as well as other forms of non-contact energy transfer. These systems have many advantages over conventional wired energy transfers, including greater safety and ease of use, reduced wear and tear, etc. In real-world charging situations, however, the ability to maintain a relation spot between the primary (transmitting) and secondary (receiving) coils is not always possible. For maximum efficiency of energy transfer between the two coils, proper alignment of the two coils must occur so that most of the magnetic field that the primary coil generates connects with the second coil. When the primary coil's alignment deviates from that of the secondary coil during operation, the ability for the two coils to achieve effective Coupling through magnetism diminishes. This condition, known as "misalignment," occurs naturally in real-life situations where electric vehicles park, because various factors contribute to lateral/forward/backward, upward/downward, angular displacements between the two coils, including tolerances on positioning, user actions/behaviours, mechanical constraints, etc [1]. When two coils that transfer power via inductive Coupling move out of alignment with each other, that is called misalignment. This misalignment has a serious effect on the performance of an IPT system because if the coils have less mutual inductance, then you will get decreased power transfer from source to load (receiver) and lower overall efficiency. Besides decreasing overall efficiency, misaligned coils can cause excessive current stress on the power electronics (inverters) as well as the compensation components [2]. The inverter may draw more reactive current to sustain its output, which results in higher losses due to conduction and switching, and this also generates more thermal stress and voltage spikes that can negatively impact the overall reliability of the IPT system over time. Therefore, for IPT systems to be functionally usable in real-world applications, there needs to be methods incorporated into them that can provide for stabilizing their operation regardless of whether the transmitting and receiving coils are aligned with each other or not. Misalignment can have a major impact on other aspects of operation other than mutual inductance [3]. One of these impacts is the effect on the coupling coefficient as a result of magnetic flux distribution variations that result in a change to the effective self-inductance of the coils. This resultant change can have an impact on resonance in the compensation network. Most IPT systems will operate at or near resonance in order to achieve maximum power transfer and to minimize reactive power circulation. If the value of inductance is changed, then

the frequency of resonance is also changed. If the operating frequency is maintained, and the resonance point drifts away from this frequency, then the system will be considered detuned. Detuning results in an increase in circulating reactive current and reduces the system's efficiency [4]. On occasion, it will degrade the zero-voltage or zero-current switching conditions. It is, therefore, important to try to maintain resonance when the coupling changes to produce stable and efficient operation. Misalignment has been known; currently, the literature provides multiple options for mitigating its adverse effects.

1.1. Literature Review

Coil geometry optimization is an explored method. Researchers try to design coils capable of producing even more uniform magnetic flux distributions and coupling coefficients that should remain relatively unchanged despite greater positional offsets by designing the physical means of transmitting and receiving coils to achieve these two goals. Possible approaches to coil geometries include circular coils, Double D (DD), and Double D Quadrature (DDQ). The design elements of these coils have purposely created a more uniform magnetic field and decreased the amount of mutual inductance sensitivity to change when the transmitting and receiving coils are moved laterally from one another [5-7].

As an example, DD and DDQ structures have resulted from the overlapping or orthogonal coil segments. This allows for both the coupling region to be larger than traditional coil designs and also increases the number of coils in both x and y planes simultaneously. Although improving tolerances to misalignments generally results from these designs, they generally provide more complex structures requiring specialized fabrication methods and usually result in higher manufacturing costs. There are numerous applications in which redesigning an entire magnetic coupler may not be practical due to space limitations, financial constraints, or requirements for standardization.

A method that is also being looked into is the dynamic adjustment of the inductance of the circuit by using variable inductors so that the circuit can compensate for misalignment due to the changes in mutual inductance [8]. The major downsides to variable inductors are that, when operating at a high frequency, the magnetic cores may saturate. If the high current is going through the wire that makes up the coil, it is likely to saturate, thus limiting the tuning range of the variable inductor as well as producing a non-linear response. Another downside is that to implement a controllable inductor, it usually requires an auxiliary DC excitation source to bias the magnetic core; thus increasing the complication and cost of the system [9-11]. As a result of these issues, variable inductors are not common in high-frequency soldering applications for IPT. Another solution that is more practical and has been investigated to a much greater extent in the IPT field is the use of Switch-Controlled Capacitors (SCCs). The Capacitor plays a critical role in determining the resonant frequency of a resonant IPT system [12]. By varying the effective value of the Capacitor, you can re-establish the resonant condition; thus, when a change is made to the value of the inductance that is associated with misaligned coils. The SCCs are usually made up of one or more semiconductor switches in addition to the use of auxiliary capacitors. By varying the duty cycle or the switching pattern, the effective capacitance that is seen by the resonant network can be changed, therefore allowing the resonant circuit to be dynamically tuned without the concerns and issues of magnetic saturation associated with variable inductors [13].

There are multiple SCC topologies available, including a basic configuration that only features one switch and one auxiliary Capacitor, either connected in parallel or series with the main compensation capacitor. While this is a very easy design, it does not necessarily provide good tuning resolution or tolerance flexibility [14]. More complicated SCC topologies with two switches and one auxiliary Capacitor have an extended second capacitance range. The downside, however, is that the more active devices that exist in a circuit, the higher the amount of switching loss and the higher the voltage stress across the semiconductor devices in the circuit. As switching frequency increases, these switching losses become significant, resulting in decreased overall efficiency. Therefore, the trade-off of a system capable of both tuning capability and switching performance is crucial [15].

Aside from misalignment tolerance, IPT charging systems need to satisfy the battery charging profiles for the energy storage devices. This includes providing both CC and CV charging. There are two main charging modes on a battery: the first mode is when CC is provided to the battery to raise the SOC rapidly, and the second mode is when the SOC reaches close to its nominal voltage and CV is supplied to ensure that the battery is not overcharged through safe operation. Therefore, an IPT system designed for battery charging must be able to deliver both CC and CV types of charging [14, 16, 17].

The LCC-S configuration is preferred due to the fewer components required on the secondary side in comparison to fully symmetrical hybrid topologies; however, adding CC/CV capabilities to these types of systems will require additional control devices or active switching devices. PWM-controlled capacitors provide an alternative means to allow compensation tuning without changing the basic network structure [18]. An approach has been developed that preserves the basic Series–Series configuration while replacing conventional series capacitors with PWM-controlled capacitors. This provides an excellent balance of simplicity and flexibility for use in power electronics. The Series-Series (SS) topology is simple and well known, with only two series inductors and two series capacitors in both the primary and secondary sides of the system. [3, 15, 19-22] When the fixed series capacitors are

replaced with PWMCC units, the system will be able to maintain dynamic resonance adjustment to compensate for changes in mutual inductance or load conditions. This approach increases the tolerance for misalignment while maintaining the structural simplicity of the system [20]. Using dynamic tuning of the capacitance, the system can restore the resonant condition as it experiences coupling variations. This allows the system to operate at either constant current or constant voltage, depending upon the charging profile [22]. In addition, since only the effective capacitance is being modified, as opposed to the entire compensation topology, the need for additional hardware is minimal compared to other, more complicated hybrid networks.

Additionally, when operating at a constant frequency, dynamic compensation will keep the resonant frequency of the system within the allowable operating range at all times [3]. To help with coil optimization and using a hybrid compensation strategy to reduce the negative effects, both types of solutions will involve higher levels of mechanical or electrical complexity. Variable inductors have practical limitations (due to saturation and control) and do not provide a practical means of tunable inductance. Use of switch-controlled capacitance (particularly in a PWM-controlled way) is an effective and flexible approach to dynamically tuning inductance. To meet the requirements of CC/CV charging, the compensation arrangement must provide both current-source and voltage-source characteristics. By utilizing PWM-controlled capacitors in a basic Series-Series compensation configuration, it is possible to create a design that allows for misalignment tolerance and the ability to provide both CC/CV functionality while maintaining structural integrity with lower complexity, and providing an IPT system with the highest efficiency possible in a unified manner [23]. Figure 1 illustrates the IPT system architecture, where AC mains are converted to high-frequency AC, transferred through magnetically coupled coils, then rectified and regulated to charge the lithium-ion battery efficiently.

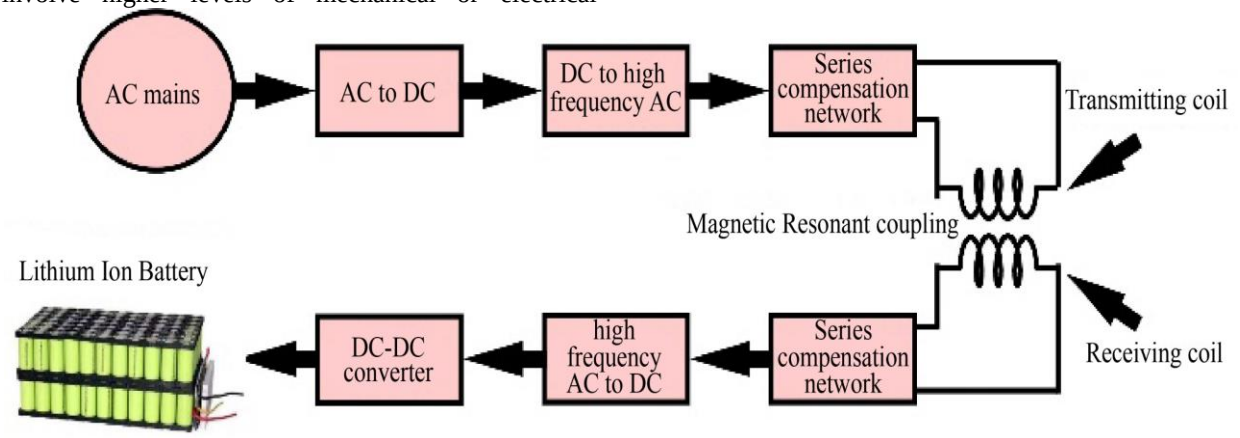

Fig. 1 IPT system block representation

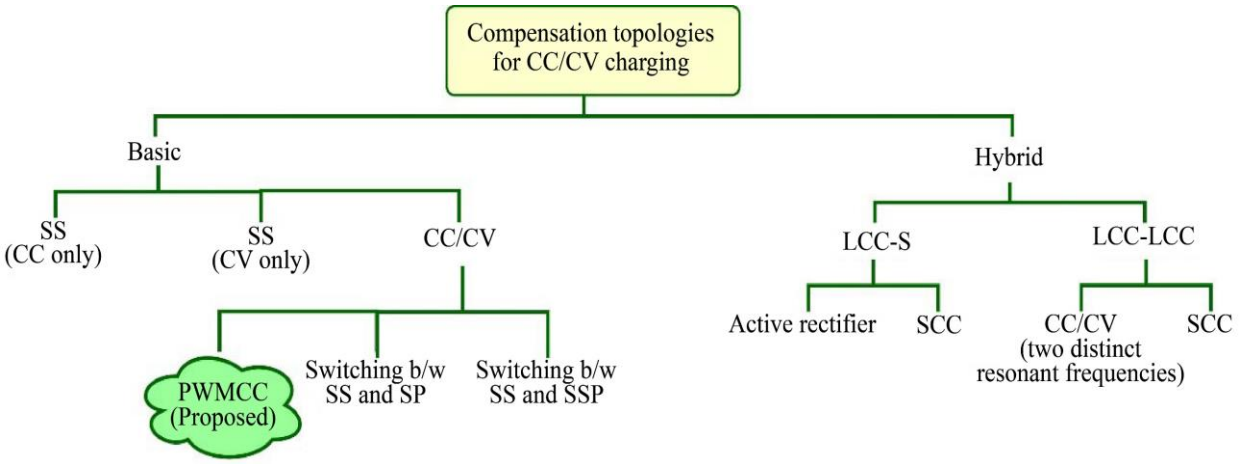

Fig. 2 CC/CV charging methods classification

1.2. Research Gaps

Currently, there are several different established Compensation Topologies used in IPT Systems to achieve (CC-CV) Charging, as shown in Figure 2; however, most of these Compensation Topologies have unique challenges, including complicated circuit structures.

- Hybrid Compensation Networks also usually increase the component count, cost, and complexity of control.
- Numerous methods utilize dual-side control or communication links, which increase the difficulty of implementation and reduce the overall reliability of the IPT System.
- Any misalignment between Transmitting and Receiving Coils directly influences mutual inductance, altering both the resonant frequency and degrading Statute Regulation.
- Coil Structure Optimization Techniques offer some level of improvement in the design tolerance, yet often necessitate complex Mechanical Designs and are impractical for Infinite IPT Systems.
- Variable Inductors and/or Frequency Shifting introduce additional Losses, concerns about saturation, and very complicated control strategies.

Although it cannot be disputed that many different methods have been reported to have accomplished either CC Operation or CV Operation independently and successfully, no method has thus far accomplished both CC Operation and CV Operation, regardless of the degree of Coupling Variation, and has also done so using very simple hardware. No verified Methods exist that have been developed to provide a simplified and fixed-frequency IPT System capable of providing load-independent CC/CV Performance under Misalignment, and that similarly utilize simple hardware. Therefore, a system that results in stable CC and CV charging operation during times of dynamic load and coupling variations will need to operate at a fixed frequency with minimal hardware complexity.

1.3. Novelty of this Work

- A Pulse-Width Modulation Controlled Capacitor (PWMCC) is added to a Series-Series (SS) compensation network and enables dynamic adjustment of effective capacitance.
- CC and CV charging are accomplished without changing the frequency; therefore, frequency shifting control schemes are avoided.
- When the coil misaligns, the PWMCC retunes the resonant condition in response to changes in mutual inductance.CC and CV outputs are stable regardless of variation in load resistance.
- Each compensation branch requires one auxiliary Capacitor and a controlled switch; thus, compared to LCC or hybrid topologies, fewer components are required.
- Coil misalignment does not require multi-coil or special magnetic structures to provide for coupling variation tolerance. Compared with conventional SCC-based tuning methods, switching loss is minimized by the use of the PWMCC configuration.
- By using capacitance adjustment instead of a structural reconfiguration, there is a smooth transition between CC and CV charging modes.
- By avoiding the use of dual-sided communication, the primary control implementation remains simple.
- The performance of the PWMCC is supported by both simulation and actual data.

In this paper, an inductive power transfer system that utilizes PWMCC as the compensation capacitor is proposed. It consists of a full bridge inverter operating at 85kHz fixed frequency, a transmitter and receiver coil, and the diode bridge rectifier. The symmetrical coil structure is adopted for its simplicity. The Popular Series-Series compensation is used. The novelty lies in the addition of the PWMCC as the compensation capacitance. In the proposed method, the switch-controlled Capacitor contains one switch and an additional capacitor [21, 22]. This allows for accurate tuning with low switching losses. The PWM-Controlled Capacitor's (PWMCC) duty cycle is adjusted to accomplish the required effective capacitance.

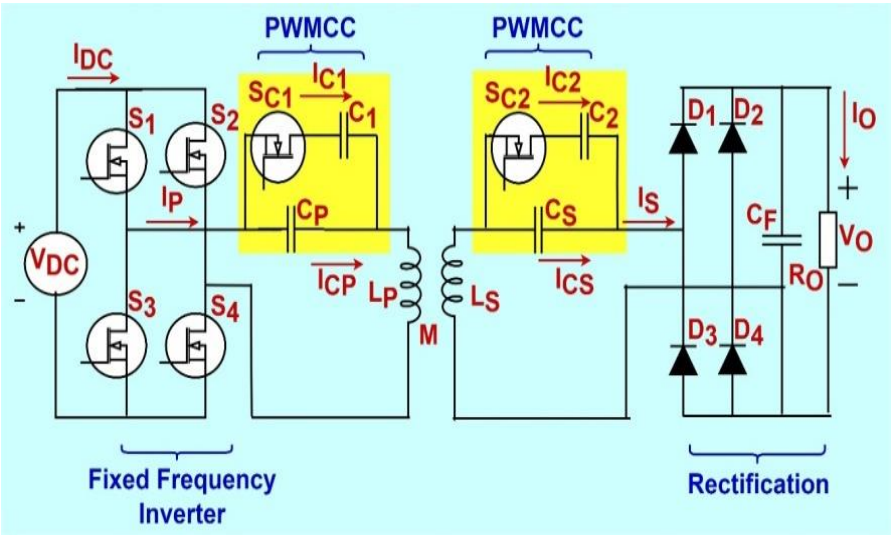

Fig. 3 Proposed inductive power transfer system

For CC operation, the capacitance is set to one specific value, while in CV mode, the capacitance is tuned to a different specific value. During Coupling and/or load variations, capacitance can dynamically be re-configured for a smooth transition between the CC and CV modes when necessary. The remaining part of the article is separated into the following sections. Section II discusses the proposed idea in detail with circuit explanation and key expressions with methodology. Section III validates the concept by simulation results. Section IV concludes the article with the future scope.

2. The Proposed IPT System

The IPT system propose has four MOSFET Switches (S_1, S_2, S_3, S_4) as the inverter stage, four Diodes (D_1, D_2, D_3, D_4) along with a filter Capacitor (C_F) as the rectifier circuit, and both a primary and secondary set of transmitting coils that each contain a PWM-Controlled Capacitor block (PWMCC) to perform compensation. This section describes the proposed IPT system, explains how the function and operating principle of a PWMCC block are applied during CC/CV operation and under conditions of coil misalignment, and concludes by discussing system specifications and coil design considerations.

2.1. Arrangement of the Hybrid Compensation WPT System

The full-bridge inverter illustrated in Figure 3 functions as a high-frequency AC power supply. For the time frame between 0 and T_s/ 2 , switches S_1 & S_4 are ON causing backwards current flow condensing through load path. Around the time frame T_s / 2 to T_s , switches S_2 & S_3 are switched ON i.e. conduct and as a result currents pass in reverse, hence producing the alternating square wave V_p. As the switching frequency synchronizes with the resonating frequency ω_R, the current on the primary side approaches sinusoidal via compensation networks. For simplification, only the base frequency component of the output voltage is analyzed since V_p contains harmonics sifted through resonating [3]. The output voltage from the inverter will be a square wave, so it can be approximated with a Fourier series by using the fundamental component only. Therefore, it can be considered that to find out how much Voltage there is coming out of the inverter, look for just the fundamental portion of it and not any harmonics, as they are basically going to disappear due to the resonance of the system. The respective equations are given below in Equations (1) and (2).

$$V_P = \sum_{n=odd}^{\infty} \frac{4V_{DC}}{n\pi} \sin n\,\omega_R t \quad (1)$$

$$V_{P1} = \frac{4V_{DC}}{\pi} \sin \omega_R\, t \quad (2)$$

The current is purely sinusoidal as obtained in Equation (3).

$$I_P = I_{PM} \sin(\omega_R t + \varphi) \quad (3)$$

Where V, is input (to the inverter) DC voltageV_{P1}, is fundamental component of the primary (inverter) output voltage I_P is current (to the inverter) through primary I_{PM} is peak current through primary inverter ϕ is the phase angle between fundamental components of the output voltage and current n is the Harmonic Order, t is Time ω_R is Switching Angular Frequency of the system (selected equal to the Resonant Frequency).

2.2. Load Independent Output Voltage

The proposed run-time IPT system utilizes a Series-Series compensation topology and has its Equivalent circuit shown in Figure 4. The T-model will be used in circuit analysis for establishing the resonant conditions in Constant Voltage (CV) Mode.

$$\omega_R = \frac{1}{\sqrt{(L_P - M)C_P}} = \frac{1}{\sqrt{(L_S - M)C_S}} \quad (4)$$

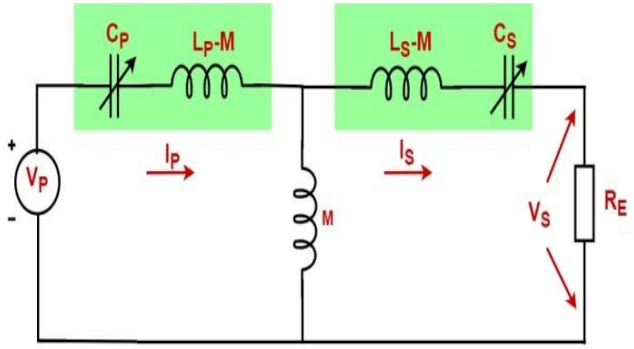

Fig. 4 T-Model for CV mode

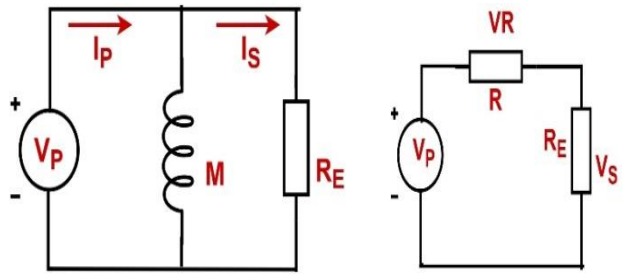

Fig. 5 Simplified model (a) reduced model ,and (b) loss model

The T-model is converted to an equivalent circuit, as shown in Figure 5. In this context, primary self-inductance L_p and the secondary self-inductance L_s represent the primary and secondary self-inductance, respectively.

The mutual inductance between the two coils is represented by M, the secondary coil current is represented by I_s, the secondary coil voltage is represented by V_s, and the reflected load resistance R_e is represented by Re. If the assumption of the resonant condition from Equation (4) can further reduce the mutual inductance, M, it would then appear as being in parallel with the reflected load resistance, R_e.

Assuming that an ideal situation and neglecting any parasitic or conduction losses, the input voltage would appear across the output resistor almost as directly as possible; therefore, we could say in Equation (5) that the input voltage will approximately equal the output voltage. Considering practical losses, it is necessary to introduce an equivalent series resistance R as shown in Figure 5. By performing the analysis of the modified circuit, Equation (6).

$$V_P = V_S \tag{5}$$

$$\frac{V_P}{V_S} = 1 - \frac{V_R}{V_S} \tag{6}$$

Where R is the cumulative resistance of the various components present in the system, V_R is the equivalent voltage drop across the various resistances in the system.

After fetching the desired resonant condition, the input impedance is merely the parallel combination of mutual inductance and Load resistance. The input impedance expression leads to three different possible cases.

Case 1 : When the load resistance is much greater than the mutual inductance, the effective input impedance is j_{XM}, which is purely inductive. The current is 90 degrees out of phase with the input voltage.

Case 2 : The Z_{in} almost becomes equal to R_E when the reactance due to the mutual inductance is much larger compared to RE. Zero power angle is achievable.

Case 3 : The phase angle lies between 90 degrees and zero degrees when neither of them is larger. By properly choosing the values, zero-voltage switching is achievable when the Z_{in} is slightly inductive.

Through the above discussion, producing a constant output voltage seems very straightforward theoretically. Nevertheless, realizing it practically is very difficult. The capacitors used for compensation would vary due to ageing, environment, and many other factors. Hence, the resonant condition is disturbed and so is the output. The graph in Figure 6 shows how much Capacitance (C) will have to be compensated for as a function of the Coupling (k_c) of the transformer for various frequencies.

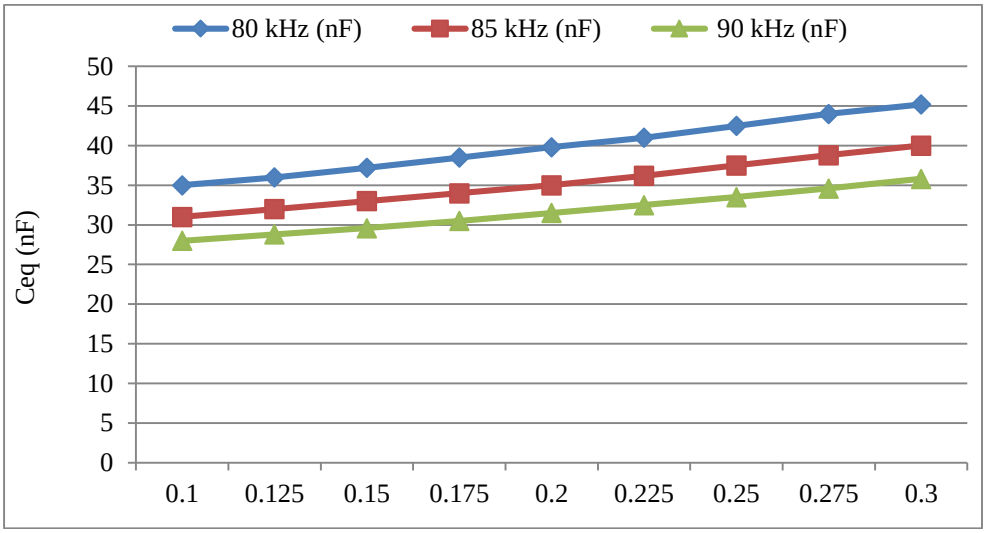

Fig. 6 Compensation capacitance for the different coupling coefficients

The needed Capacitance (C) varies smoothly as the coupling Coefficient (k_c) or the switching Frequency (f) changes. The input current is calculated using Equation (7), because the transformer does not have any series components to convert an equivalent circuit to an input current.

$$I_P = \frac{V_P}{\left[\frac{(R_E \times j\omega_R M)}{(R_E + j\omega_R M)}\right]} \tag{7}$$

$$I_S = \frac{I_P \times j\omega_R M}{(R_E + j\omega_R M)} \tag{8}$$

$$\left(\frac{I_S}{V_P}\right) = \frac{1}{R_E} \tag{9}$$

To calculate the output current (i.e., to find the load current), you will need to use the current division shown in Equation (8). The output of the transformer (primary voltage (V_p) to secondary current (I_s) is defined using Equation (9) and is related to the load Resistance (R_O). If the load resistance is increased, the output (I_s) is decreased, and vice versa. This means that you can always take the input voltage and adjust it according to the desired output current (Is) for changes in the output current.

2.3. Current is Constant, Independent of Load

The circuit explaining constant current mode operation is shown in Figure 7. By using the series-series compensation network T model shown in Figure 7(a), the proposed IPT

system is obtained. The T model is solved to obtain the resonant condition for the CC mode given in (10).

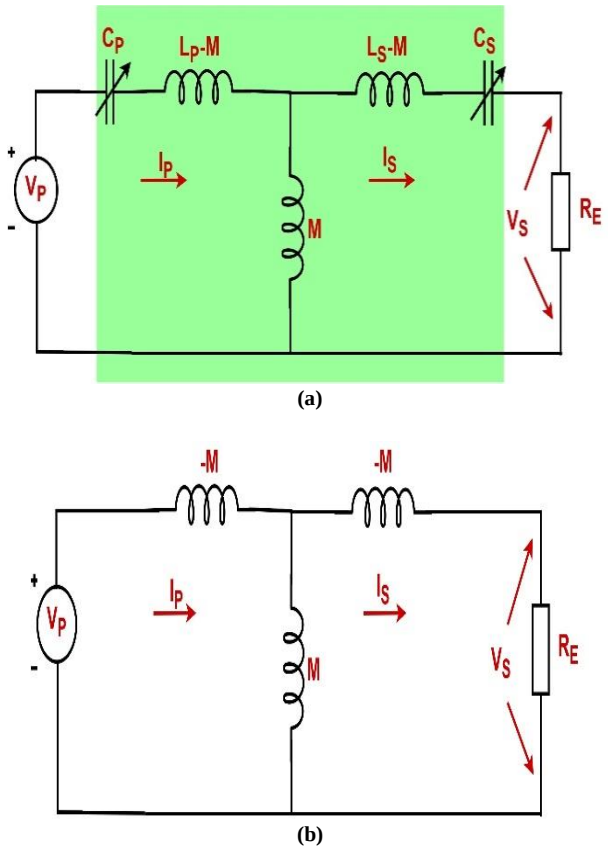

Fig. 7 Constant current mode (a) T-model, and (b) reduced model

Using circuit theory, Figure 7(b) is utilized to get the input impedance Z_{IN} expression written in Equation (11). As Z_{IN} has real components only, a unity power factor is achieved during constant current charging. Using Equation (11). Equation (12) is derived.

Subsequently, using the current division rule in Figure 7(b), Equation (13) is computed. The secondary current I_S in Equation (14) confirms that the current is no longer a function of R_O. Thus, the constant current charging process is ensured when complying with Equation (10). Equation (15) gives the expression for V_S/V_P.

$$\omega_R = \frac{1}{\sqrt{L_P C_P}} = \frac{1}{\sqrt{L_S C_S}} \quad (10)$$

$$Z_{IN} = \frac{\omega^2 M^2}{R_E} \quad (11)$$

$$I_P = \frac{V_P}{\left(\frac{\omega^2 M^2}{R_E}\right)} \quad (12)$$

$$I_S = I_P \left(\frac{j\omega M}{R_E + j\omega M - j\omega M}\right) (13)$$

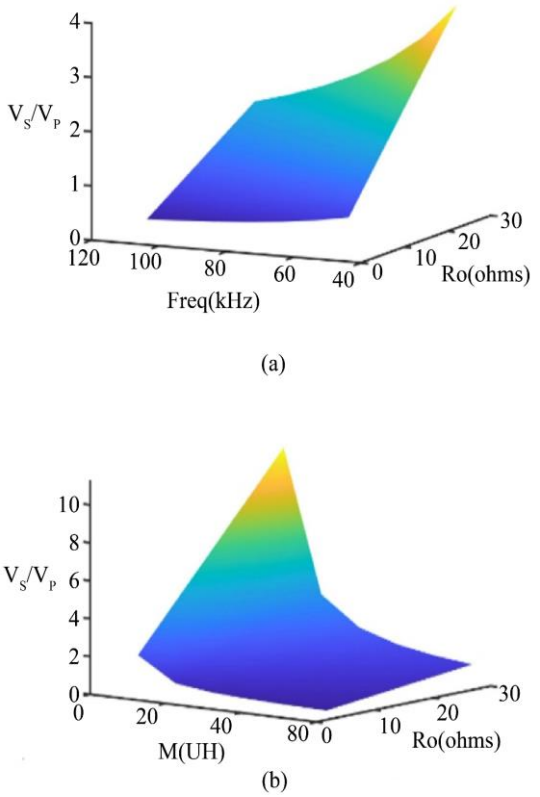

Fig. 8 V_S/V_P Curve for (a) change in frequency and R_O, (b) change in M and R_O

$$I_S = \frac{V_P}{j\omega M} \quad (14)$$

$$\frac{V_S}{V_P} = \frac{\omega^2 M^2 - (8/\pi^2) R_O j\omega M}{\omega^2 M^2} \quad (15)$$

Figure 8(a) shows the output voltage gain (V_S/V_P) for various loads and variations in switching frequency. The effect of various loads and Mutual Inductance (M) on the output voltage gain (V_{DS}/V_P) is illustrated in Figure 8(b). The 3D plot in Figure 8 shows the extent to which V_S/V_P reaches when quantities are manoeuvred. The R_O has a greater influence on the V_S/V_P because it increases when the R_O increases, as shown in Figure 8(a). Furthermore, the M and F have little impact on V_S/V_P. If M or F varies, there is only a subtle variation in V_S/V_P as shown in Figure 8(b). However, when both M and F increase or decrease together, V_S/V_P gets significantly affected.

2.4. PWM Controlled Capacitor

The PWM-Controlled Capacitor (PWMCC) has been very popular in resonant converters to achieve better performance. The PWMCC can act as a variable capacitor with the help of one additional Capacitor and a MOSFET switch, as shown in Figure 9. The series combination of the MOSFET (S_{C1}) and the auxiliary Capacitor (C_1) of the compensation network is connected in parallel to the main Capacitor (C_X). The output capacitance is adjusted to provide

the desired compensation by changing the duty cycle of MOSFET S_{C1} as described in Equation (16). A suitable capacitor value can be computed for any variation in mutual inductance or operating frequency using Equation (17).

$$C_{eq} = C_X\left(\frac{2\alpha C_1}{C_X + C_1(1-2\alpha)} + 1\right) \quad (16)$$

$$\omega_R = \frac{1}{\sqrt{(L_P - M)C_{P_{eq}}}} = \frac{1}{\sqrt{(L_S - M)C_{S_{eq}}}} \quad (17)$$

Where C_{eq} is the equivalent capacitance, C_X is the Primary/secondary compensation capacitance, C_1 is the auxiliary capacitance, α is the duty cycle of the PWMCC, and C_{Peq}/C_{Seq} are the Primary/Secondary equivalent capacitance.

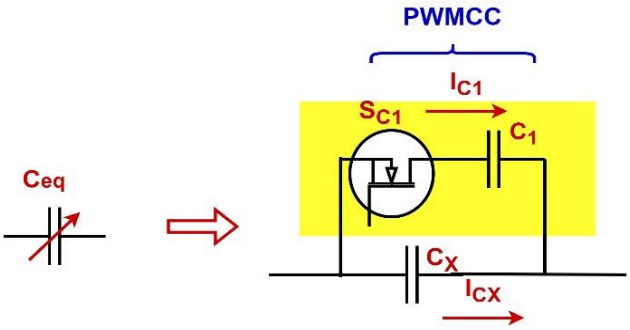

Fig. 9 PWM controlled capacitor as a variable capacitor

2.5. Misalignment Tolerance

When there is coupling variation, the resonant operation for the CC or CV is disturbed. Consequently, the effect on input current and the output voltage during CV operation can be given by the following Equations (18) and (19).

$$I_{P1} = \frac{V_P}{\frac{(R_E + j\Delta X_{LS})X_M j}{R_E + jX_M + j\Delta X_{LS}} + j\Delta X_{LP}} \quad (18)$$

$$\frac{V_S}{V_P} = \frac{\left(1 - \frac{j\Delta X_{LP}}{\frac{(R_E + j\Delta X_{LS})X_M j}{R_E + jX_M + j\Delta X_{LS}} + j\Delta X_{LP}}\right) \times R_E}{R_E + j\Delta X_{LS}} \quad (19)$$

$$\Delta C_p = \frac{1}{\omega_R\left(\omega_R \Delta L_p - \frac{1}{\omega_R C_P}\right)} - C_P \quad (20)$$

Where X_M is the reactance of mutual inductance, $\Delta L_P/\Delta L_S$ is the small change in the transmitter and secondary inductances, and $\Delta X_{LP}/\Delta X_{LS}$ is the change in the reactance of the same, ΔC_P is the small change in the compensation capacitance. When (L_P-M) changes by a small quantity ΔL_P, the resultant change in the capacitor value ΔC_P can be given by Equation (20). For all changes in the M, the resonant condition and V_O are influenced. Therefore, to retrieve the CV operation, the duty cycle of the PWMCC is controlled-Equations (21) and (22) state the relationship between α and M.

$$C_X\left(\frac{2\alpha C_1}{C_X + C_1(1-2\alpha)} + 1\right) = \frac{1}{\omega_R{}^2(L_X - M)} \quad (21)$$

$$\alpha = \left(\frac{(C_X + C_1) - C_X\omega_R{}^2(L_X - M)(C_X + C_1)}{2C_1}\right) \quad (22)$$

The equivalent capacitance curve is shown in Figure 10. Figure 10(a) is the 3D plot showing the effect of M and F on the desired C_{eq}. The impact of F is more visible than the impact of M. Figure 10(b) shows the impact of the duty cycle of PWMCC on the value of the equivalent capacitance. For fine-tuning, a small auxiliary capacitor is needed, and for higher variations, a larger auxiliary Capacitor is needed.

The mutual inductance (M) does not significantly affect the behavior of the inverter when it operates in the constant current mode. However, the output current magnitude (Io) is inversely related to the mutual inductance(M). In order to maintain a constant output current, the PWM signals of the inverter are appropriately modulated as shown in Figure 11. The positive and negative pulse widths of the PWM signal can be modulated symmetrically, as shown in Figure 11(a).

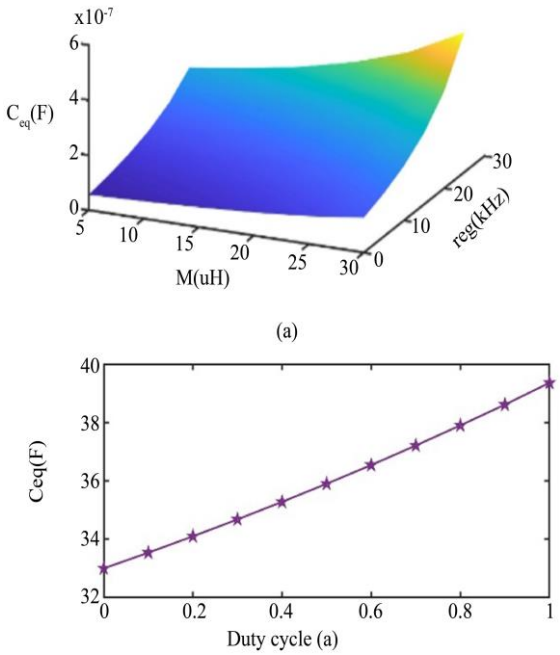

Fig. 10 Equivalent capacitance curve (a) function of mutual Inductance and operating frequency, (b) function of duty cycle

The expression for the inverter output voltage as a function of the control angle (β) is given in Equations (23) and (24), where Equation (24) represents the fundamental component of the output voltage used in the analysis that follows. To ensure CC output, every change in the mutual inductance should be addressed by the change in the positive and negative pulse width of the inverter output V_P, i.e, changing β. Equations (25) and (26) disclose the relationship between β and I_S.

$$V_P = \sum_{n=ODD}^{\infty} \frac{4V_{DC}}{n\pi} \cos(n\beta) \sin(n\omega_R t) \tag{23}$$

The output current $I_{O,}$ also has a significant role in deciding the β. As long as the required I_O is low, the β covers a large coupling variation at CC operating mode, as shown in Figure 11(b). However, the ability of the B shrinks for larger I_O. Therefore, to address the aforementioned problem, the other parameters can be controlled to maintain the CC mode operation. To maintain load-independent CC/CV output, the key parameters should be designed to obtain the desired resonant condition. Equations (15), (25), and (26) are used to obtain the required V_{DC}. The operating frequency of 85kHz is chosen as it is mostly used for IPT systems [1-3].

Figure 12 shows the system parameters design and coil geometry for a circular shape coil structure, which makes sense from two points of view: it is very simple and easy to make the same size for primary and secondary coils, which are shown in Figure 12(a). The use of Equations (27), and (28) gives the self-inductances and mutual inductance to be optimized as per [23], thus providing an optimal configuration for each configuration.

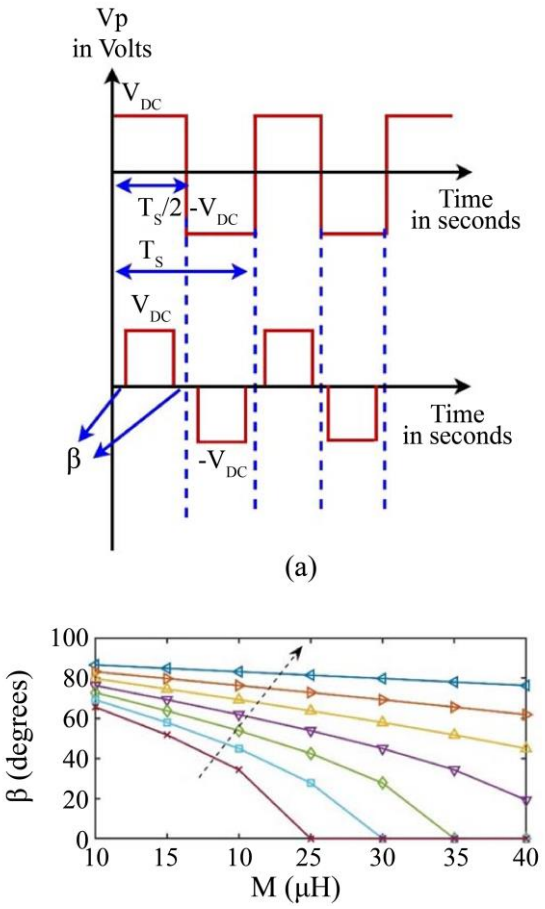

Fig. 11 Input voltage control (a)waveform, (b) control angle "β" as a function of mutual inductance

$$V_{P1} = \frac{4V_{DC}}{\pi} \cos(\beta) \sin(\omega_R t) \tag{24}$$

$$I_S = \frac{2\sqrt{2}V_{DC} \cos(\beta)}{\omega M \pi} \tag{25}$$

$$\beta = \cos^{-1}\left(\frac{I_S \omega M \pi}{2\sqrt{2}V_{DC}}\right) \tag{26}$$

2.6. Design of Parameters

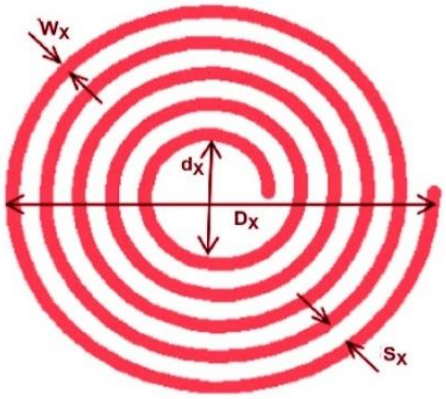

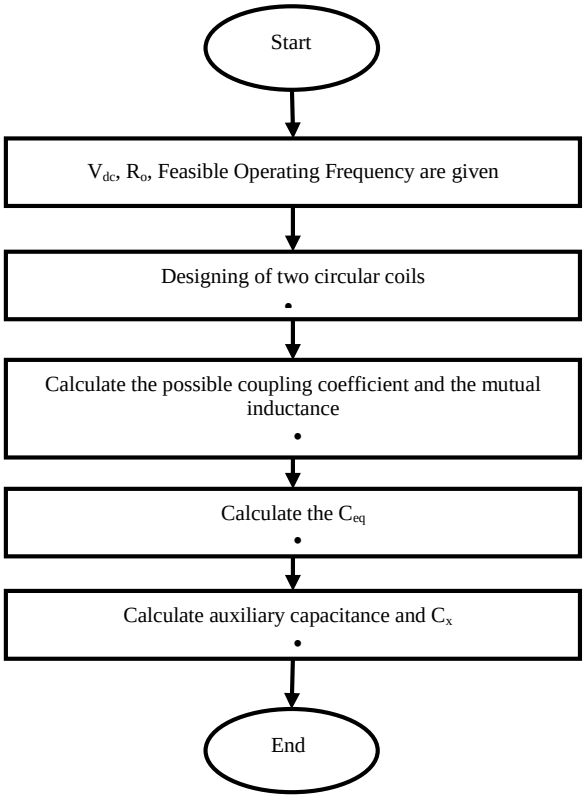

Fig. 12 Circular coil and parameter design flow chart

$$\left.\begin{aligned} L_X &= \frac{A_2 {N_P}^2}{8A+11C} \\ A &= R_X + \frac{N_X}{2}(W_X + S_X) \\ C &= N_X(W_X + S_X) \end{aligned}\right\} \quad (27)$$

$$\left.\begin{aligned} L_M &= \sum_{P=1}^{N_P}\sum_{S=1}^{N_S} 2\mu_O \frac{\sqrt{R_P R_S}}{K_{PS}}\left\{\left(1-\frac{{K_{PS}}^2}{2}\right)K_{PS}(k) - E_{PS}(k)\right\} \\ {K_{PS}}^2 &= \frac{4\alpha}{(1+\alpha)^2} + \beta^2 \\ \alpha &= \frac{R_P}{R_S} \\ \beta &= \frac{H}{R_P} \end{aligned}\right\} \quad (28)$$

Where,
R_X, d_X- coil inner radius/diameter
W_X-coil copper track width
S_X- Coil track separation
N_X- No. of coil turns
H= gap between the center of the two coils

In the calculations performed for the coil's inductance parameters, a number of elliptic integrals must be evaluated. KPS(K) and EPS(K) represent these complete elliptic integrals, which are necessary for calculating the inductance of a coil. The separation distance between each of the coils can then be used to determine the mutual inductance and Coupling. After determining the key parameters for each coil configuration as shown in Figure 12(b), the compensation capacitance values for each configuration, or Mode CC and Mode CV, can be computed using Equations (10) and (4), respectively. After determining the target capacitance values for each mode, Equation (16) is used to calculate the corresponding ratio of capacitance between the primary and secondary capacitors, $C_P/$. Also, to calculate the ratio of the auxiliary capacitors, C_1/C_2

3. Results and Discussion

The specifications given in Table 1 are used for the simulation study. Initially, the coupling coefficient is fixed at 0.2. With K=0.2, the capacitor values 28.09nF for CC mode and 35.07nF for CV mode are identified from (10) and (4), respectively. For testing the misalignment tolerance, the coupling coefficient is allowed to vary between 0.12 and 0.24.

Table 1. Parameter values

Parameters	Symbol	Values
Input voltage	V_{in}	100V
Primary coil self-inductance	L_P	125µH
Primary Resistance	R_p	0.1Ω
Secondary coil self-inductance	L_s	125µH
Secondary Resistance	R_s	0.1Ω
Primary main /auxiliary capacitance	C_p	30nF/5nF
Secondary main /auxiliary capacitance	C_s	30nF/5nF
Bridge rectifier filter	C_f	100µF
Switching frequency	ω_S	85KHz
Resonant Frequency	ω_R	85KHz

3.1. Simulation Results

For examining the misalignment tolerance of the proposed system, mutual inductance (M) is varied between 15µH and 30µH. As the Coupling between the coils varies, the PWMCC continuously changes its value to maintain CV mode, as shown in Figure 15. Without PWMCC, V_O increases or decreases based on coupling strength. Figure 15 (a), (b), and (c) confirm that the CV mode is sustained during the tuned state, irrespective of the value of M. Figure 16 shows V_O and I_O for both CV and CC modes.

In Figure 16(a), though the voltage is supposed to be constant in CV mode, there is a negligibly small variation in the V_O. The same is the case for I_O in Figure 16(b), irrespective of the CC mode. Nevertheless, the variations are neglected as they are very small. Figure 17 compares the value of V_O with and without tuning conditions in CV mode. Through simulation results, it is noted that the PWMCC finely tunes the compensation capacitance value in order to keep the operation in either CC or CV mode, irrespective of the misalignment. This method achieves the desired result using simple manipulation of the compensation capacitance in the series-series compensation network.

3.2. Experimental Verification

The setup of experiments illustrated in Figure 18 is based on the IPT system outlined in Figure 2. The IPT stage will operate at 85kHz. The inverter will use high-frequency MOSFETs with the appropriate gate driver circuits. A controller board, an FPGA Spartan-6, implements the control algorithm and generates the MOSFET gate pulses. A sufficient deadline will be introduced to ensure that the inverter operates safely. The input voltage is provided by a programmable DC power supply. The wireless power transfer is accomplished using two identical coils. A Mixed-Signal Oscilloscope (MSO) is used to measure the parameters

needed, with voltage probes and current probes connected to the circuit. The MSO waveforms for V_P, I_P, $V_O$and I_O during CC mode are shown in Figure 19. The output current remains almost constant at 6.2 A regardless of load transitions (see Figure 19(a), (b), and (c)). During this time, the coupling coefficient maintains a constant value of .2; thus, only slight output current variations occur from 2-5% as the load varies, while voltage changes accordingly to adjust to keep the current level constant. The experimental waveforms from the proposed SS-IPT system's operation in CV mode are illustrated in Figure 20.

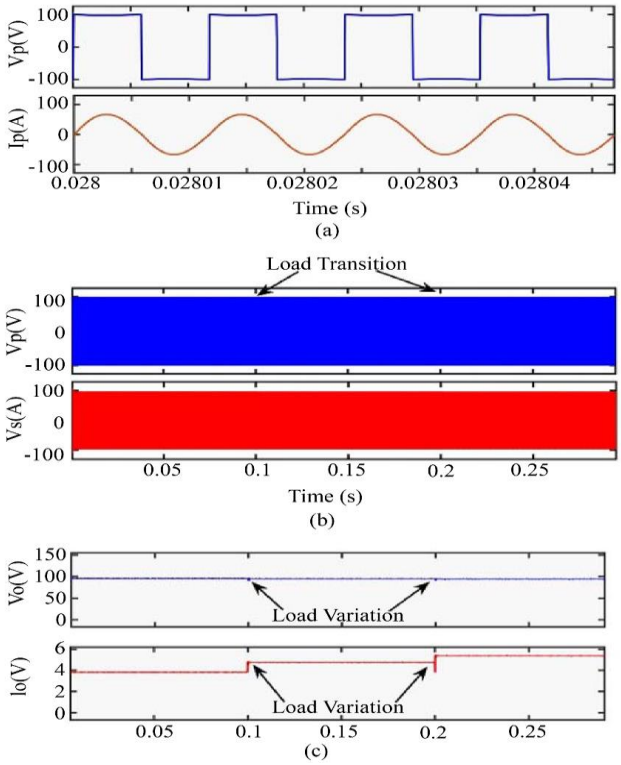

Fig. 13 Waveforms during constant voltage mode (a)Voltage and current of transmitter (b) Primary and receiver voltage, (c) Output voltage and current

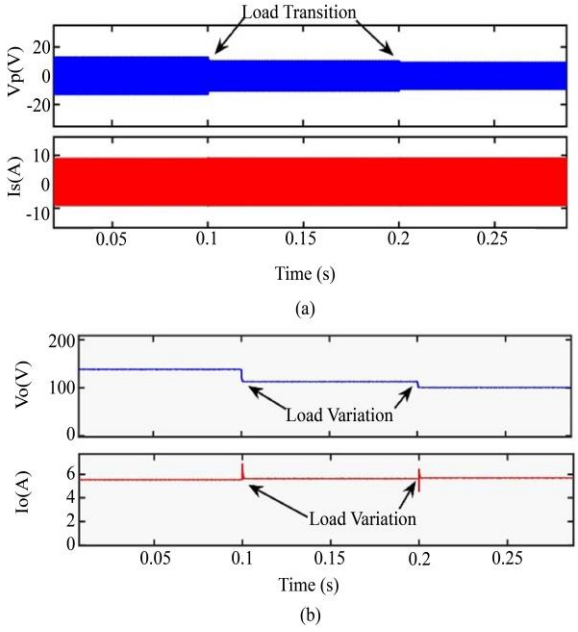

Fig. 14 waveforms during constant current mode (a) Primary and secondary current, (b) Current and voltage at the output

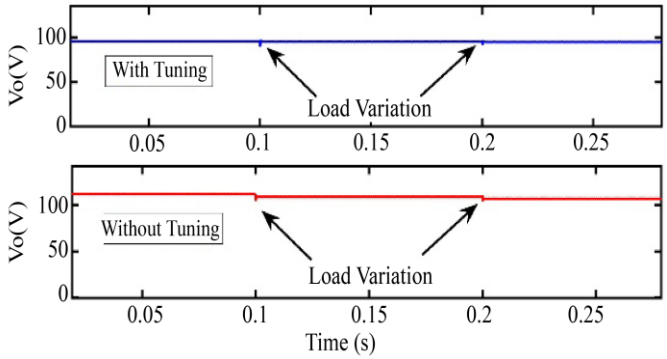

(a)

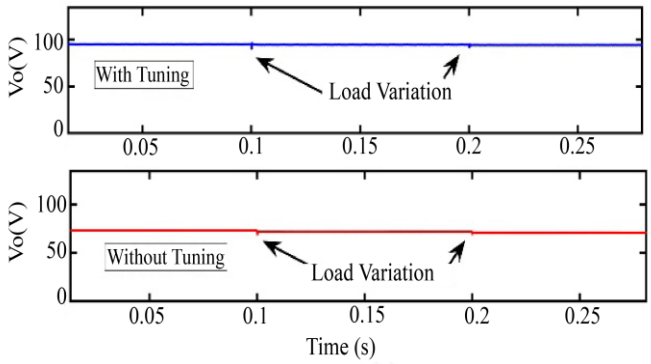

(b)

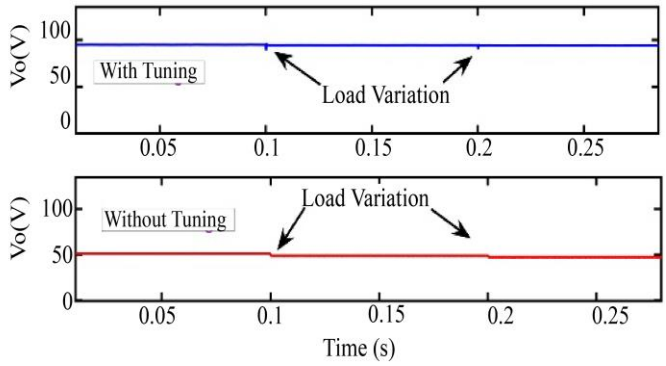

(c)

Fig. 15 Output voltage under varying load resistance, with and without tuning: (a) for K=0.24, (b) for K=0.16, and (c) for K=0.12

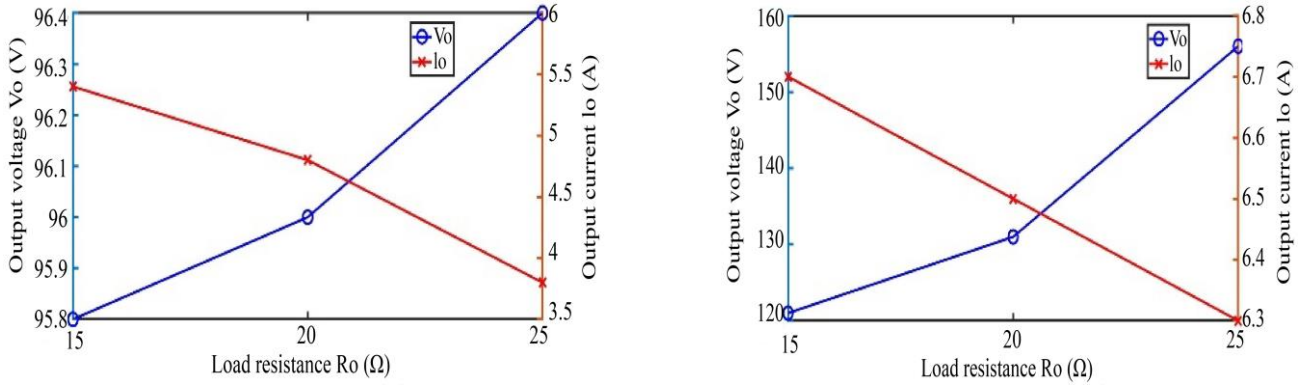

(a) **(b)**

Fig. 16 Output voltage and output current for different values of load resistance (a) during cv mode, and (b) during cc mode

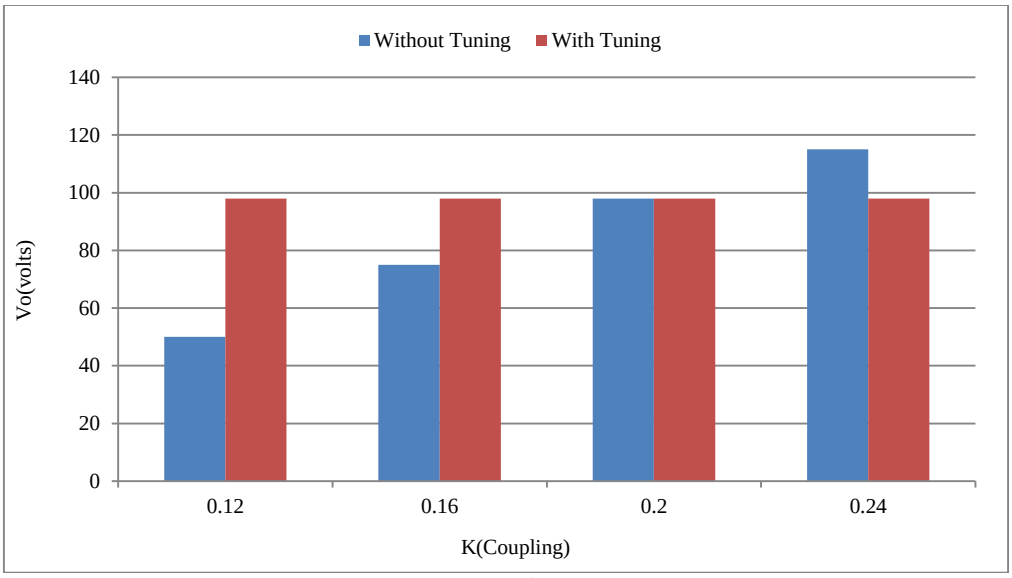

Fig. 17 Output voltage before and after tuning

The experiment shows the output voltage of the SS-IPT system is maintained at almost 87 volts for all tested load resistances when the coupling coefficient is 0.20 (i.e., output voltage is constant for 0 to 100% load change). For varying loads on the SS-IPT system, the output voltage is stable at around 87 volts as load resistance increases from 10 ohms to 20 ohms and then from 20 ohms to 30 ohms. Also shown are the changes in output current as the system responds to the changing output power due to changing load resistances (shown in Figures 20(a), 20(b), and 20(c)). The experimental waveforms for the SS-IPT system operating at 30 Ω in CC mode, as per Figure 19(a), show that while the output voltage of the inverter has a square waveform, the primary currents are very close to being sinusoidal, as designed, because of resonant operation, occurring at the appropriate frequency. The output voltage, V_O, will rapidly increase in order to supply sufficient power to the load based on load requirements. With an increase in V_O, the current I_O, will maintain a level that's substantially unchanged from that which was required of it before V_O increased.

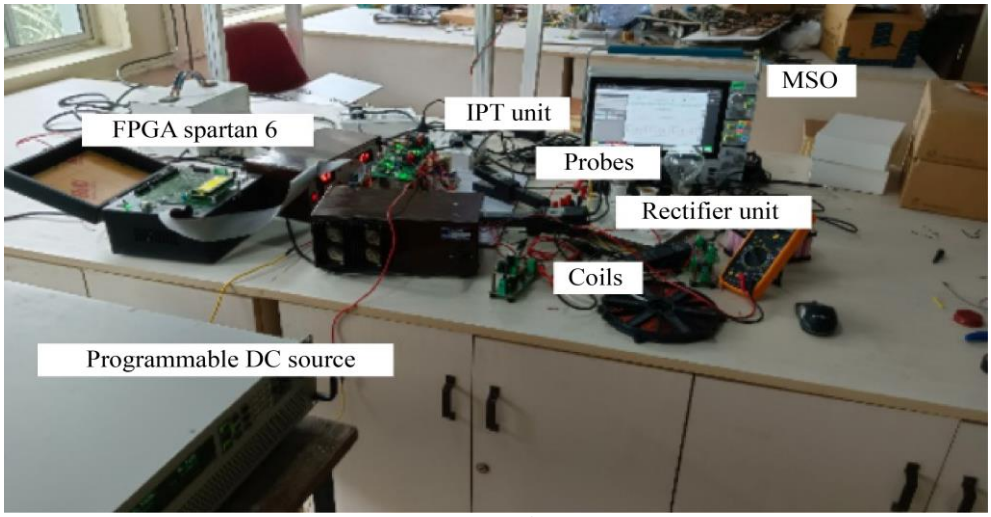

Fig. 18 Hardware setup of the Proposed IPT

Thus confirming that with the change in V_O, the CC operation of the SS-IPT system has been maintained due to the system uses automatic output adjustment based on load requirements. It is also apparent that the stable current waveform reflects good tuning and regulation of the compensation network and inverter operation, and that the proposed PWMCC-based IPT system will provide for the continuous delivery of constant-current performance under higher load resistance, without distortion or instability.

The CC-mode output waveforms of the inverter are illustrated in Figure 19(b) at an output resistance of 20 Ω. The

Inverter Voltage (V_P) still behaves as a high-frequency square wave. The Primary Current (I_P) remains sinusoidal since it is at resonance. As the load resistance is decreased, the output Voltage (V_O) Will Also Decrease To Maintain A Constant Output Current. The measured output current (I_O) remains close to its reference value, indicating effective current regulation. Hence, this behavior demonstrates that the CC operation is load independent, as the inverter and compensation network dynamically change the voltage level, so that the current magnitude will not be affected. The smoothness of the current waveform, along with a stable output, shows that the system is well-tuned and that the capacitance operating under PWM control maintains constant current under varying load resistances. CC mode operates at reduced load resistance level (10Ω) as shown in Figure 19(c).

With the output voltage (V_O) decreasing more to compensate for a lower load, the output waveform from the inverter is still a square wave. However, the primary current waveform (I_P) continues to have a sinusoidal shape due to the effects of resonance filtration. (I_O) remains essentially constant, demonstrating that the system provides effective regulation of the load current over a wide range of load resistances, therefore demonstrating that CC mode is unaffected by changes in load since the output voltage automatically varies to maintain the target load current. The experimental data confirm the practicality of using the PWMCC-based compensation technique to accomplish consistent current delivery in low-resistance load conditions.

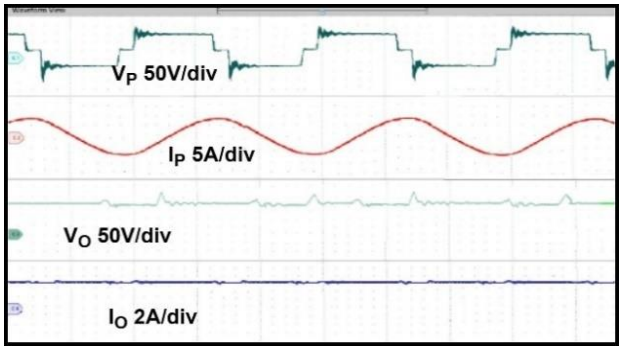

(a)

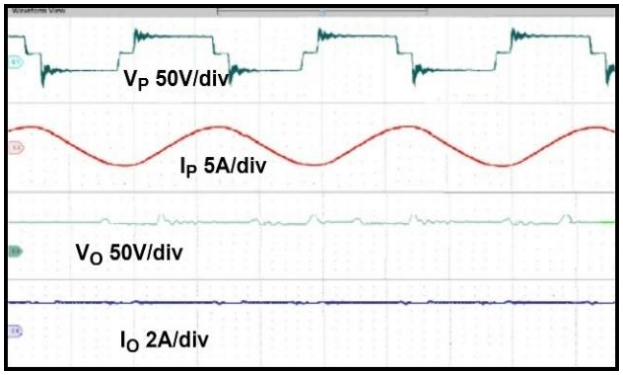

(b)

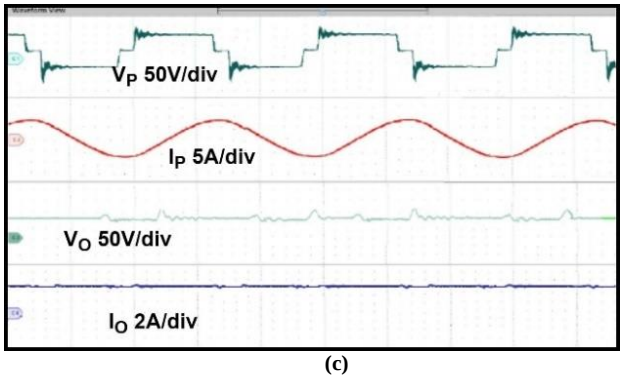

(c)

Fig. 19 In CC mode (a) V_P, I_P, V_O, and I_O waveforms for R=30Ω (b) V_P, I_P, V_O, and I_O waveforms for R=20Ω, and (c) V_P, I_P, V_O, and I_O waveforms for R=10Ω

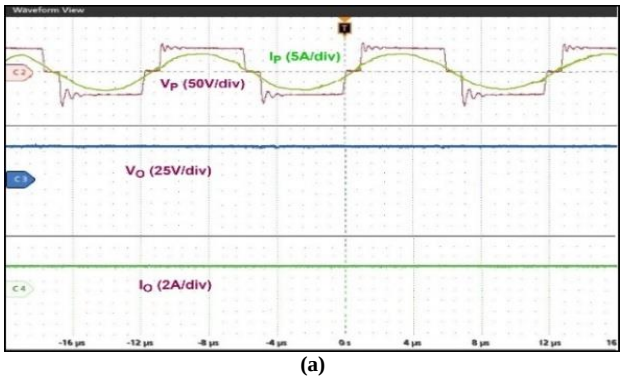

(a)

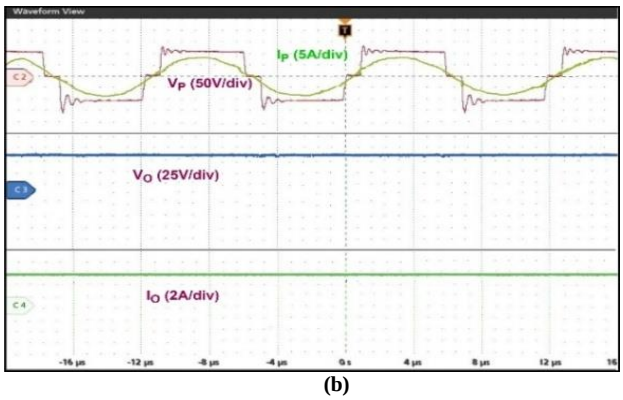

(b)

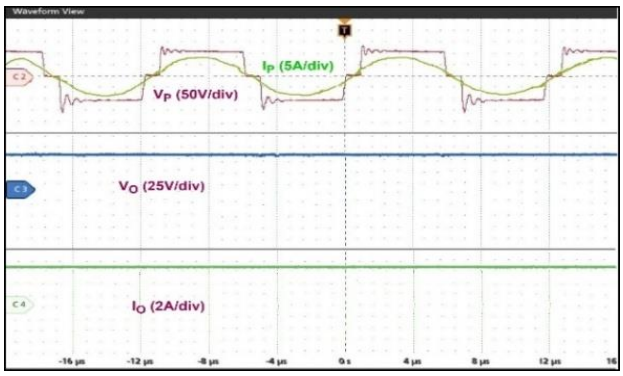

(c)

Fig. 20 In CV mode (a) V_P, I_P, V_O, and I_O waveforms for R=30Ω (b) V_P, I_P, V_O, and I_O waveforms for R=20Ω, and (c) V_P, I_P, V_O, and I_O waveforms for R=10Ω

The IPT system from Figure 20(a) illustrates the experimental waveforms when working in constant voltage (CV) mode with a resistance of 10 ohms. The inverter output voltage V_P is a high-frequency square wave, and the primary current V_P*I_P is sinusoidal. The output voltage V_O is fixed and regulated, demonstrating that the system is working properly in a CV mode. Because of the low resistance, the current output I_O is relatively high to satisfy the load. The stable voltage waveform demonstrates that the compensation network is tuned properly for CV operation. As expected in a charging application, the system produces a consistent output voltage while allowing the output current to fluctuate with the load. The voltage and current (inverting) waveforms in CV mode at 20 Ω load resistance can be seen in Figure 20(b). The inverter voltage and primary current are expected to be square and sinusoidal, respectively, with the output Voltage (V_O) remaining almost at the same target level, indicating that good voltage regulation has occurred. When the load resistance is increased, the output Current (I_O) decreases due to the lower demand for power. This behavior indicates that CV mode is operating appropriately and that voltage is maintained while current varies based on load conditions. The waveforms illustrate stable system operation and successful control of the PWMCC compensation network for different loads. In Figure 21, the output Voltage (V_o) is shown for the range of the coupling coefficient K varying from 0.25 to 0.16.

Table 2. Comparison between the proposed system and similar approaches

Article	No of coils	Compensation Network	Additional Switches	Number of L and C Components	Misalign-ment Tolerance	K Independent CC/CV Operation	ZVS Operation	ZPA
Proposed	2	S-S	2	2 capacitors	yes	yes	yes (CV)	yes(CC)
[21]	4	S-LCC & S-S	4	4 capacitors 2 inductors	yes	no	yes	no
[15]	2	LCC-S	2	3 capacitors 1 inductor	No	yes	no	no
[13]	2	S-S & S-P	2	2 capacitors	No	yes	yes	no
[14]	2	S-S & S-SP	2	3 capacitors	Yes	yes	no	no
[14]	2	LCC-S	2	3 capacitors 1 inductor	No	no	no	Yes
[16]	2	LCC-LCC	nil	5 capacitors 2 inductors	yes	yes	no	No
[22]	4	S-S	nil	2 capacitors, magnetic coupler	yes	yes	yes (CV)	yes (CC)
[10]	2	S-S	nil	2 variable inductor	no	yes	yes	no

The primary voltage, Vp, and the primary current, Ip, show no significant changes, indicating that there is still constant excitation from the inverter side. While the output voltage waveform will show a noticeable shift and slight time delay from the previous values, the reduction of magnetic Coupling (K) will have an effect on the power transfer capabilities of the transmitter and receiver coils, causing a slight dynamic deviation before the system stabilizes. The area of enhanced delay highlights the sensitivity of output performance to variation of the Coupling in the wireless power transfer system. For misalignment issues, the PWMCC, unlike the previous cases, must be active all the time. As soon as there is a deviation in V_O, the duty cycle of the PWMCC is updated by the closed-loop mechanism to prevent changes in V_O. For experimental demonstration, the K is changed from 0.25 to 0.16, and the response of V_O is recorded in Figure 21. The proposed system improves performance through the addition of a PWMCC to a basic SS compensation topology, enabling dynamic resonance tuning without changing the operating frequency or requiring complex hybrid compensation systems. Other current technologies provide misalignment tolerance and CC/CV functionality using either complex coil geometries (DD and DDQ) or multi-order compensation topologies (LCC-S and LCC), which typically have additional manufacturing costs associated with their higher magnetic complexity, increased component count, and control requirements.

In contrast, our method maintains a simple circular coil structure using a basic SS network, reducing overall hardware complexity while providing comparable functionality. Another reason for improved performance in the proposed system is that it is able to adjust the effective compensation capacitance in real-time using PWMCC instead of a fixed capacitor. In conventional SS systems using fixed capacitors, any variation in the mutual inductance due to misalignment causes a change in the resonant condition, which leads to detuning and an increase in reactive current and decreased efficiency.

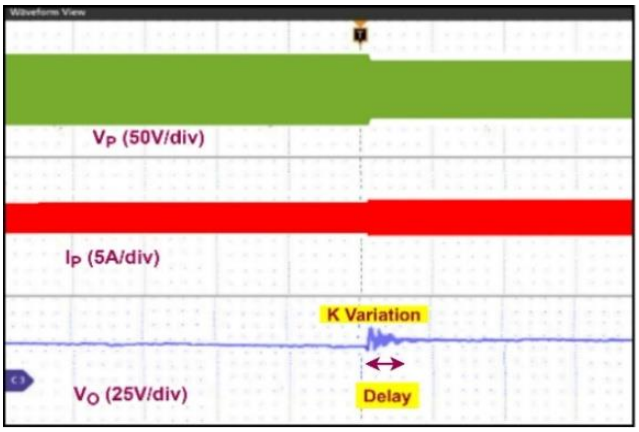

Fig. 21 V_O for K (0.25 & 0.16)

The proposed system restores resonance as coupling conditions vary by dynamically adjusting the effective capacitance. Therefore, this continuous tracking of resonance provides a direct improvement of efficiency while limiting the amount of reactive power that circulates and the amount of stress on the devices as compared to fixed-compensation systems. Unlike variable inductors, where magnetic core saturation and DC bias circuits must be considered, the use of PWMCC provides a linear and precise method of controlling effective capacitance by modulating the duty cycle. The rapid dynamic response provided by PWMCC is also able to offer better tuning precision than variable inductors at high frequency. In contrast with hybrid compensation schemes (such as LCC-LCC), which utilize two resonant frequencies to achieve current control and constant voltage, the proposed solution allows for operation at a constant frequency. This eliminates instability due to varying the frequency of the switch and simplifies the inverter design, improves the electromagnetic compatibility of the inverter system, and avoids the efficiency losses caused by changing the switching frequency from one point in time to another.

In addition, hybrid systems increase conduction losses and parasitic losses due to requiring more inductors and capacitors. By using the same SS circuit topology while electronically modifying only the effective capacitance, the proposed solution minimizes both the number of passive components required and their associated losses. One more benefit is the effortless implementation of both current and voltage constant modes without the need to physically change the compensation network.

In previously published systems, the use of extra MOSFETs to switch between SS and SP configurations resulted in higher switching stress and control complexity. The effective capacitance of an inverter is adjusted so that both current and voltage constant modes can be implemented without problems. Experimental results also further confirm the improved reliability against coupling variations; during experimentation, output voltage/current deviation was minimal as the coupling coefficient was changed within the range tested.

Conversely, fixed-compensation systems listed in the literature display high amounts of output fluctuation when exposed to similar amounts of misalignment. PWMCC uses closed-loop control of the PWM signal to rapidly correct any differences in azimuthal distance from the inverting transformer, therefore reducing the settling time and avoiding extended distortion. Furthermore, the reduced number of components in this off-axis coil configuration compared to that of higher-order compensation arrangements decreases the switching and conduction losses.

Fewer passive components decrease the overall number of parasitic resistances and stray inductances present, thereby increasing overall circuit efficiency and reliability. The circular symmetrical coils contribute to ease of mechanical design; thus, it is expected that they will enhance the practical application of this technology for real-world electric vehicle charging systems.

4. Conclusion

In this article, PWMCC-based Series-Series compensation is introduced in the IPT system for CC/CV battery charging applications with high misalignment tolerance. The PWMCC smoothly changes the compensation capacitance to the optimum value for ensuring CC or CV mode based on the load requirement. The mutual inductance is varied dynamically to show the ability of PWMCC for misalignment.

It has been demonstrated through simulation and experimental results that the PWMCC maintains the operation in CC mode at 6.2A and during CV mode at 87V irrespective of the load variations. The tuning ability keeps the operation stable for misalignment problems. The ability of the PWMCC to get the desired capacitance precisely to keep the operation in the necessary mode makes it superior to other proposed methods. However, the distortions and deviations are settled in a period of 100ms to restore the VO into the CV mode.

The comparison is carried out between the proposed system and the other similar systems based on the CC/CV operation and misalignment tolerance as listed in Table 2. The basic series-series compensation is one of the main advantages of the proposed system when compared to the other systems [13-16, 21] with higher-order compensation networks. The proposed system allows smooth variation of capacitance using PWMCC during coupling variation to keep the system in resonance continuously. The switching losses and stress of the PWMCC are lower compared to those used in [14]. The L and C components involved in the proposed IPT system are much less compared to [14-16, 21]. The circular coil of the same geometry is chosen, unlike the other works [10, 22] involving additional coils, making the mechanical arrangement difficult.

Acknowledgments

The authors gratefully acknowledge the Wireless Charging Research Centre, Department of Electrical and Electronics Engineering, SRM Institute of Science and Technology, Kattankulathur-603203, India, for providing access to the essential components and equipment necessary for this research, supported by the Council of Scientific & Industrial Research (CSIR), India, under the Extramural Research-II (EMR II) scheme, Grant 22/0901/23/EMR-II. We also extend our appreciation for the facilities and support rendered by the Microcontroller Lab, Department of Electrical and Electronics Engineering, SRM Institute of Science and Technology, Kattankulathur-603203, India.

References

[1] Siqi Li, and Chunting Chris Mi, "Wireless Power Transfer for Electric Vehicle Applications," *IEEE Journal of Emerging and Selected Topics in Power Electronics*, vol. 3, no. 1, pp. 4-17, 2015. [CrossRef] [Google Scholar] [Publisher Link]

[2] Devendra Patil et al., "Wireless Power Transfer for Vehicular Applications: Overview and Challenges," *IEEE Transactions on Transportation Electrification*, vol. 4, no. 1, pp. 3-37, 2018. [CrossRef] [Google Scholar] [Publisher Link]

[3] Guanxi Li, and Hao Ma, "A Hybrid IPT System with High-Misalignment Tolerance and Inherent CC-CV Output Characteristics for EVs Charging Applications," *IEEE Journal of Emerging and Selected Topics in Power Electronics*, vol. 10, no. 3, pp. 3152-3160, 2022. [CrossRef] [Google Scholar] [Publisher Link]

[4] Van-Binh Vu et al., "Operation of Inductive Charging Systems under Misalignment Conditions: A Review for Electric Vehicles," *IEEE Transactions on Transportation Electrification*, vol. 9, no. 1, pp. 1857-1887, 2023. [CrossRef] [Google Scholar] [Publisher Link]

[5] Lei Zhao et al., "A Misalignment Tolerant Series-Hybrid Wireless EV Charging System with Integrated Magnetics," *IEEE Transactions on Power Electronics*, vol. 34, no. 2, pp. 1276-1285, 2019. [CrossRef] [Google Scholar] [Publisher Link]

[6] Mickel Budhia et al., "Development of a Single-Sided Flux Magnetic Coupler for Electric Vehicle IPT Charging Systems," *IEEE Transactions on Industrial Electronics*, vol. 60, no. 1, pp. 318-328, 2013. [CrossRef] [Google Scholar] [Publisher Link]

[7] Kai Song et al., "Design of DD Coil with High Misalignment Tolerance and Low EMF Emissions for Wireless Electric Vehicle Charging Systems," *IEEE Transactions on Power Electronics*, vol. 35, no. 9, pp. 9034-9045, 2020. [CrossRef] [Google Scholar] [Publisher Link]

[8] Xiaohui Qu et al., "A Family of Hybrid IPT Topologies with Near Load-Independent Output and High Tolerance to Pad Misalignment," *IEEE Transactions on Power Electronics*, vol. 35, no. 7, pp. 6867-6877, 2020. [CrossRef] [Google Scholar] [Publisher Link]

[9] Yong Li et al., "Extension of ZVS Region of Series-Series WPT Systems by an Auxiliary Variable Inductor for Improving Efficiency," *IEEE Transactions on Power Electronics*, vol. 36, no. 7, pp. 7513-7525, 2021. [CrossRef] [Google Scholar] [Publisher Link]

[10] Xiao Zhu et al., "High-Efficiency WPT System for CC/CV Charging based on Double-Half-Bridge Inverter Topology with Variable Inductors," *IEEE Transactions on Power Electronics*, vol. 37, no. 2, pp. 2437-2448, 2022. [CrossRef] [Google Scholar] [Publisher Link]

[11] Zhicong Huang et al., "A Single-Stage Inductive-Power-Transfer Converter for Constant-Power and Maximum-Efficiency Battery Charging," *IEEE Transactions on Power Electronics*, vol. 35, no. 9, pp. 8973-8984, 2020. [CrossRef] [Google Scholar] [Publisher Link]

[12] Fei Xu, Siu-Chung Wong, and Chi K. Tse, "Overall Loss Compensation and Optimization Control in Single-Stage Inductive Power Transfer Converter Delivering Constant Power," *IEEE Transactions on Power Electronics*, vol. 37, no. 1, pp. 1146-1158, 2022. [CrossRef] [Google Scholar] [Publisher Link]

[13] Kai Song et al., "Constant Current/Voltage Charging Operation for Series-Series and Series-Parallel Compensated Wireless Power Transfer Systems Employing Primary-Side Controller," *IEEE Transactions on Power Electronics*, vol. 33, no. 9, pp. 8065-8080, 2018. [CrossRef] [Google Scholar] [Publisher Link]

[14] Chi Shing Wong et al., "Design of High-Efficiency Inductive Charging System with Load-Independent Output Voltage and Current Tolerant of Varying Coupling Condition," *IEEE Transactions on Power Electronics*, vol. 36, no. 12, pp. 13546-13561, 2021. [CrossRef] [Google Scholar] [Publisher Link]

[15] Van-Binh Vu, Duc-Hung Tran, and Woojin Choi, "Implementation of the Constant Current and Constant Voltage Charge of Inductive Power Transfer Systems with the Double-Sided LCC Compensation Topology for Electric Vehicle Battery Charge Applications," *IEEE Transactions on Power Electronics*, vol. 33, no. 9, pp. 7398-7410, 2018. [CrossRef] [Google Scholar] [Publisher Link]

[16] Jingang Li, Xuze Zhang, and Xiangqian Tong, "Research and Design of Misalignment-Tolerant LCC-LCC Compensated IPT System with Constant-Current and Constant-Voltage Output," *IEEE Transactions on Power Electronics*, vol. 38, no. 1, pp. 1301-1313, 2023. [CrossRef] [Google Scholar] [Publisher Link]

[17] Zhimeng Liu et al., "Primary-Side Linear Control for Constant Current/Voltage Charging of the Wireless Power Transfer System based on the LCC-N Compensation Topology," *IEEE Transactions on Industrial Electronics*, vol. 69, no. 9, pp. 8895-8904, 2022. [CrossRef] [Google Scholar] [Publisher Link]

[18] Cheng Chen et al., "Modeling and Decoupled Control of Inductive Power Transfer to Implement Constant Current/Voltage Charging and ZVS Operating for Electric Vehicles," *IEEE Access*, vol. 6, pp. 59917-59928, 2018. [CrossRef] [Google Scholar] [Publisher Link]

[19] Veli Yenil, and Sevilay Cetin, "Load Independent Constant Current and Constant Voltage Control of LCC-Series Compensated Wireless EV Charger," *IEEE Transactions on Power Electronics*, vol. 37, no. 7, pp. 8701-8712, 2022. [CrossRef] [Google Scholar] [Publisher Link]

[20] Qiang Zhao et al., "The Load Estimation and Power Tracking Integrated Control Strategy for Dual-Sides Controlled LCC Compensated Wireless Charging System," *IEEE Access*, vol. 7, pp. 75749-75761, 2019. [CrossRef] [Google Scholar] [Publisher Link]

[21] Hailong Zhang et al., "A Hybrid Compensation Topology with Single Switch for Battery Charging of Inductive Power Transfer Systems," *IEEE Access*, vol. 7, pp. 171095-171104, 2019. [CrossRef] [Google Scholar] [Publisher Link]

[22] Zhenjie Li et al., "Constant Current/Voltage Charging for Primary-Side Controlled Wireless Charging System without using Dual-Side Communication," *IEEE Transactions on Power Electronics*, vol. 36, no. 12, pp. 13562-13577, 2021. [CrossRef] [Google Scholar] [Publisher Link]

[23] Ravi Kumar Yakala et al., "Optimization of Circular Coil Design for Wireless Power Transfer System in Electric Vehicle Battery Charging Applications," *Transactions of the Indian National Academy of Engineering*, vol. 6, no. 3, pp. 765-774, 2021. [CrossRef] [Google Scholar] [Publisher Link]